Reliability Engineering and System Safety 218 (2022) 108166

Contents lists available at ScienceDirect

Reliability Engineering and System Safety

journal homepage: www.elsevier.com/locate/ress

Degradation and reliability of multi-function systems using the hazard rate matrix and Markovian approximation

Daoqing Zhou [a], C.P. Sun [a,b], Yi-Mu Du [a], Xuefei Guan [a,*]

[a] Graduate School of China Academy of Engineering Physics, Beijing 100193, China
[b] Beijing Computational Science Research Center, Beijing 100193, China

ARTICLE INFO

Keywords:
Reliability
Hazard rate matrix
Markovian approximation
Multi-function systems
Degradation process

ABSTRACT

The study presents a new method to model the degradation and reliability of multi-function complex systems using the hazard rate matrix and Markovian approximation. The system is hierarchically decomposed into a set of states according to the states of its functions, and the hazard rate matrix is proposed to describe the failure rates of the functions. By using Markovian approximation, the elements of the hazard rate matrix can be expressed as a set of dynamical equations involving the failure information about the functions. Consequently, the dynamical behavior of the degradation for the whole system and its functions can be determined using the observed failure data of those functions instead of the lifetime data of the whole system, eliminating the need for lifetime testing data of the whole system in statistical-based reliability assessment. The overall method is illustrated using an example problem, and is further applied to a power system degradation problem to demonstrate its usage in realistic engineering applications.

1. Introduction

Degradation is a common process in the fields of physics, engineering, biology, and so on. The degradation under uncertainty is closely related to the concept of reliability, which is defined as a probabilistic measure to characterize the ability to perform the intended functions for a specified period of time in a defined environment [1]. Early studies on reliability assessment can be traced back to the 1950s [2,3]. The statistical analysis of failure time data is used to describe the lifespan of electronic components, and a full understanding of the aging mechanism is limited. Relying on the law of large numbers, it requires a sufficient amount of lifetime data to estimate the hazard rate accurately [4–7]. By fitting the lifetime data to a prescribed distribution using methods such as maximum likelihood estimate and method of moments, the hazard rate associated with the distribution is derived. Probabilistic inference can alternatively be used to construct the lifetime distribution given the lifetime data and obtain the corresponding hazard rate function [8,9]. Rational approaches to probabilistic inference on the optimal distribution and hazard rate functions include Bayesian methods [10–13] and entropy-based methods [14–16].

Direct modeling of the hazard rate of the whole system can be difficult for many high-reliability demanding complex systems with longer lifespans. For one thing, it can be unrealistic to obtain statistically sufficient lifetime data in a short time. Although accelerated life testing can be used [17–19] to reduce the lifetime data, the facilities are usually designed for testing components and sub-systems, and its application to a whole complex system with a larger physical dimension is rarely possible. For another, treating the system as a whole for reliability assessment provides limited understanding of the dependence between participating components and sub-systems, and reveals less information on the weak spots for reliability growth. System decomposition and network modeling are widely-used approaches to model the reliability of a complex system [20–22]. The complex system under consideration is decomposed into a set of relatively independent sub-systems or units whose reliabilities can be assigned or derived. The network represents the possible routes to the required function, allowing for using the basic probability rules and theorems to obtain the reliability of the system [23–25]. To derive or assign the reliability of independent sub-systems or units, statistical, empirical, and physical models can be used, for examples, in the fields of materials [26–30], electronics [31,32], and many others [33–37]. In Refs. [38,39], a MaxEnt approach is developed to obtain the optimal hazard rate function, and a double-function system is demonstrated using the linear assumption. For more complex systems, the linear assumption may be invalid, thus limiting its applications in realistic problems.

This study develops a new method to model the degradation behavior and reliability of complex systems. The system is abstracted as a set of states which are determined by the functions of the system.

* Corresponding author.
E-mail addresses: ymdu@gscaep.ac.cn (Y.-M. Du), xfguan@gscaep.ac.cn (X. Guan).

https://doi.org/10.1016/j.ress.2021.108166
Received 26 June 2021; Received in revised form 15 September 2021; Accepted 23 October 2021
Available online 6 November 2021
0951-8320/

The hazard rate matrix is proposed to describe the degradation of the functions. In this context, the focus is to restore the degradation of the system using observable information on the functions, which is an inverse problem in nature. The dynamical behavior of the degradation of a system refers to the time-dependent variation of the system state, and is essentially characterized by the hazard rate matrix of the system. By incorporating the Markovian approximation, the equations for each of the elements in the hazard rate matrix can be formulated, and subsequently be solved using failure information on the functions. The rate of degradation in general depends on the state of the system. In the scope of the method, the dependence is dealt with in two aspects. The influence of other correlated functions on a specific function is explicitly incorporated as the non-diagonal elements in the hazard rate matrix. In addition, the dependence is implicitly encoded in the observable lifetime data of the functions which are used when solving the hazard rate equations. The method is not focused on the mechanism-based modeling and simulations regarding the degradation of the functions and their correlations, which have been discussed elsewhere in detail, for example, in Refs. [40–42].

The proposed method is different from the physical component-based modeling methods. In these methods, the system reliability model is built upon the participating components and their cascading and logical relationship. The evaluation of the system reliability in such cases is a forward problem in nature, and requires component-wise information such as the lifetime distributions of the components. In addition, the influence of other components on a particular component can be quantitatively intractable in a system. By leveraging the hazard rate matrix and state-based modeling approach, such detailed information, which may rarely be available for complex high-reliability-demanding systems, is not required in the proposed method. The method provides a means to estimate the degradation behavior of the system based on the observable failure information on its functions with the following potential advantages. For one thing, it eliminates the need for lifetime testing data on the whole system in conventional statistical lifetime data analysis approach. For another, it can alleviate the difficulty in quantifying the degradation of a component contributed by other influencing components in component-based modeling methods.

The remainder of the study is organized as follows. First, the hazard rate matrix for multi-function systems is introduced, and reducible and irreducible hazard rate matrices are derived, respectively. The relationship between the matrix components and the conditional probabilities of the state transition is signified. Next, the dynamical equations of the elements of the hazard rate matrix is formulated using Markovian approximation. The degradation process of a multi-function system and its functions can be resolved by solving the dynamical equations. Following that, a three-function system is used to illustrate the method, and the accuracy of the results obtained by the proposed method is verified. The developed method is further applied to a realistic engineering problem. Finally conclusions are drawn.

2. Hazard rate matrix of multi-function systems

In the context of modeling multi-function systems, the term 'function' is defined by component states as detailed in Ref. [43]. Given the lifetime T with uncertainty, the reliability function $R(t)$ is defined as $R(t) = \Pr(T \geq t)$, $t \in (0, +\infty)$. The corresponding PDF for lifetime $T = t$ is expressed as $p(t) = -\mathrm{d}R(t)/\mathrm{d}t$. The hazard rate function of a single-function system $\lambda(t)$ can be expressed by the reliability function and its PDF as

$$\lambda(t) \equiv -\frac{1}{R(t)}\frac{\mathrm{d}R(t)}{\mathrm{d}t} = \frac{p(t)}{R(t)}. \tag{1}$$

For a multi-component system, the definition of structure function is not unique. A system characterized by more than one structure functions is defined as a multi-function system. According to the specific engineering requirements, each function has a corresponding failure criterion. The relationship between failure criteria of functions depends on requirements, which can be correlated or independent. Denote the reliability of function i $(i = a, b, \ldots, n)$ in an n-function system as $R_i(t)$. For such a system, the hazard rate function of the system is generalized to an n-dimensional square matrix. According to Eq. (1), the system-level reliability function $\mathbf{R}(t)$ can be expressed as

$$\frac{\mathrm{d}\mathbf{R}}{\mathrm{d}t} = -\lambda\mathbf{R}, \tag{2}$$

where $\mathbf{R} = (R_a, R_b, \ldots, R_n)^{\mathrm{T}}$ and λ is an n-by-n hazard rate matrix. It should be noted that λ is an upper triangular matrix due to the non-increasing property of reliability function $R_i(t)$.

For a general multi-function system, the relation between functions needs to be determined first. When the failure of function a can lead to the failure of function b and the failure of function b has no effect on function a, such a relation between functions a and b is denoted as $a \succ b$. As an example, consider a flashlight consisting of two light bulbs denoted as L_1 and L_2. The function a denotes the event that the flashlight can emit light; therefore, it can be one of the three states: (1) both L_1 and L_2 work properly, (2) L_1 works and L_2 fails, and (3) L_1 fails and L_2 works. When the function b denotes the event that L_1 works, the relation between a and b in this case is represented as $a \succ b$.

Table 1
The 2^n states of a fully reducible n-function system.

State	Function a	Function b	⋯	Function n
1	Work	Work	⋯	Work
2	Work	Work	⋯	Breakdown
⋮	⋮	⋮	⋱	⋮
$n+1$	Breakdown	Work	⋯	Work
⋮	⋮	⋮	⋱	⋮
2^n	Breakdown	Breakdown	⋯	Breakdown

2.1. A fully reducible n-function system

A fully reducible system means each of the functions has no effect on the other functions. It can be seen that a fully reducible n-function system has a total number of 2^n different states, as listed in Table 1. The initial conditions for the reliability of the ith function $R_i(0), i \in (a, \ldots, n)$ when the system is in states $2, \ldots, (n+1)$ in Table 1 can be expressed as

$$\begin{bmatrix} R_a(0) \\ R_b(0) \\ \vdots \\ R_n(0) \end{bmatrix} = \begin{bmatrix} 1 \\ 1 \\ \vdots \\ 0 \end{bmatrix}, \ldots, \begin{bmatrix} R_a(0) \\ R_b(0) \\ \vdots \\ R_n(0) \end{bmatrix} = \begin{bmatrix} 0 \\ 1 \\ \vdots \\ 1 \end{bmatrix}. \tag{3}$$

For initial states from 2 to $(n+1)$, $\mathrm{d}R_i/\mathrm{d}t, i \in (a, \ldots, n)$ are

$$\begin{aligned} \frac{\mathrm{d}R_n}{\mathrm{d}t} &= \lambda_{na}R_a(t) + \lambda_{nb}R_b(t) + \cdots + \lambda_{nn}R_n(t) = 0, \\ &\vdots \\ \frac{\mathrm{d}R_a}{\mathrm{d}t} &= \lambda_{aa}R_a(t) + \lambda_{ab}R_b(t) + \cdots + \lambda_{an}R_n(t) = 0. \end{aligned} \tag{4}$$

It is noted that for each of the functions, both $\mathrm{d}R_i(t)/\mathrm{d}t$ and $R_i(t)$ approach zero simultaneously due to the non-increasing and non-negativity property of $R_i(t)$. The hazard rate matrix of a fully reducible system must be diagonal; otherwise, one or more equations in Eq. (3) will violate the above conditions in Eq. (4). The hazard rate matrix λ in this case is

$$\lambda = \begin{bmatrix} \lambda_{aa} & 0 & \cdots & 0 \\ 0 & \lambda_{bb} & \cdots & 0 \\ \vdots & \vdots & \ddots & \vdots \\ 0 & 0 & \cdots & \lambda_{nn} \end{bmatrix}. \tag{5}$$

A fully reducible n-function system reduces to a total number of n single-function systems.

Table 2
The $n+1$ states of an irreducible n-function system.

State	Function a	Function b	⋯	Function n
1	Work	Work	⋯	Work
2	Work	Work	⋯	Breakdown
⋮	⋮	⋮	⋱	⋮
$n+1$	Breakdown	Breakdown	⋯	Breakdown

Table 3
Three states of an irreducible double-function system.

State	Function a	Function b
1	Work	Work
2	Work	Breakdown
3	Breakdown	Breakdown

2.2. An irreducible n-function system

In an irreducible n-function system, the relationship among the functions is $a \succ b \succ \cdots \succ n$. The $(n+1)$ different states of an irreducible n-function system are listed in Table 2. The initial conditions for the reliability of the ith function of the system, $R_i(t=0)$, can be expressed as

$$\begin{bmatrix} R_a(0) \\ R_b(0) \\ \vdots \\ R_n(0) \end{bmatrix} = \begin{bmatrix} 1 \\ 1 \\ \vdots \\ 0 \end{bmatrix}, \ldots, \begin{bmatrix} R_a(0) \\ R_b(0) \\ \vdots \\ R_n(0) \end{bmatrix} = \begin{bmatrix} 0 \\ 0 \\ \vdots \\ 0 \end{bmatrix}, \tag{6}$$

when the system is in states 2, …, $(n+1)$ in Table 2. The terms $\mathrm{d}R_i/\mathrm{d}t, i \in (a,\ldots,n)$ in this case are

$$\begin{aligned} \frac{\mathrm{d}R_n}{\mathrm{d}t} &= \lambda_{na}R_a(t) + \lambda_{nb}R_b(t) + \cdots + \lambda_{nn}R_n(t) = 0, \\ &\vdots \\ \frac{\mathrm{d}R_a}{\mathrm{d}t} &= \lambda_{aa}R_a(t) + \lambda_{ab}R_b(t) + \cdots + \lambda_{an}R_n(t) = 0. \end{aligned} \tag{7}$$

Since the reliability function $R_i(t)$ is non-increasing, $\mathrm{d}R_i/\mathrm{d}t$ and R_i approach zero simultaneously. The hazard rate matrix λ of an irreducible n-function system is an upper triangular matrix, which is expressed as

$$\lambda = \begin{bmatrix} \lambda_{aa} & \lambda_{ab} & \cdots & \lambda_{an} \\ 0 & \lambda_{bb} & \cdots & \lambda_{bn} \\ \vdots & \vdots & \ddots & \vdots \\ 0 & 0 & \cdots & \lambda_{nn} \end{bmatrix}. \tag{8}$$

2.3. Hazard rate matrix and conditional probabilities

An irreducible double-function (a and b) system is taken as an example to relate the elements of the hazard rate matrix to the conditional probabilities of the system. For $a \succ b$, the three possible states are given in Table 3. The hazard rate matrix in this case is

$$\lambda = \begin{bmatrix} \lambda_{aa} & \lambda_{ab} \\ 0 & \lambda_{bb} \end{bmatrix}. \tag{9}$$

For simplicity, alphabet suffices and numerical suffices are used to represent functions and states, respectively. From Table 3, it is known $R_a = R_1 + R_2$ and $R_b = R_1$. For all functions, $R_j(t+\Delta t) = \sum_i P(j, t+\Delta t \mid i, t)R_i(t)$, where $P(j, t+\Delta t \mid i, t)$ represents the probability that the system is in state j at time $(t+\Delta t)$ conditional on the system being in state i at time t. The PDFs of the failure times for functions a and b are expressed, respectively, as

$$\begin{aligned} p_a &= -\lim_{\Delta t\to 0}\frac{R_a(t+\Delta t) - R_a(t)}{\Delta t} \\ &= -\lim_{\Delta t\to 0}\frac{[P(1,t+\Delta t \mid 1,t) + P(2,t+\Delta t \mid 1,t)]R_1(t)}{\Delta t} \\ &\quad - \lim_{\Delta t\to 0}\frac{[P(1,t+\Delta t \mid 2,t) + P(2,t+\Delta t \mid 2,t)]R_2(t) - [R_1(t)+R_2(t)]}{\Delta t}, \text{ and} \\ p_b &= -\lim_{\Delta t\to 0}\frac{R_b(t+\Delta t) - R_b(t)}{\Delta t} \\ &= -\lim_{\Delta t\to 0}\frac{P(1,t+\Delta t \mid 1,t)R_1(t) - R_1(t)}{\Delta t}. \end{aligned} \tag{10}$$

Without considering the system-level recovery (renewal), it is noted that the conditional probability $P(1, t+\Delta t \mid 2, t) = 0$ in Eq. (10) as the transition from state 1 to state 2 is irreversible.

On the other hand, combining Eqs. (1) and (2), the PDFs of the functions can be written as

$$\begin{bmatrix} p_a \\ p_b \end{bmatrix} = \begin{bmatrix} \lambda_{aa} & \lambda_{ab} \\ 0 & \lambda_{bb} \end{bmatrix} \begin{bmatrix} R_a \\ R_b \end{bmatrix}. \tag{11}$$

Substitute p_a and p_b expressed in Eq. (10) into Eq. (11) to obtain the elements of the hazard rate matrix

$$\begin{aligned} \lambda_{aa}(t) &= \lim_{\Delta t\to 0}\frac{1 - P(2,t+\Delta t \mid 2,t)}{\Delta t}, \\ \lambda_{ab}(t) &= \lim_{\Delta t\to 0}\frac{P(2,t+\Delta t \mid 2,t) - P(1,t+\Delta t \mid 1,t) - P(2,t+\Delta t \mid 1,t)}{\Delta t}, \\ \lambda_{bb}(t) &= \lim_{\Delta t\to 0}\frac{1 - P(1,t+\Delta t \mid 1,t)}{\Delta t}. \end{aligned} \tag{12}$$

More generally, extending this formula to an n-function irreducible system, the element of the hazard rate matrix can be expressed as

$$\lambda_{ij} = \begin{cases} \lim_{\Delta t\to 0}\dfrac{1 - P(n-i+1, t+\Delta t \mid n-i+1, t)}{\Delta t}, & i = j \\ \lim_{\Delta t\to 0}\dfrac{\sum_{k=n-j+2}^{n-i+1} P(k, t+\Delta t \mid n-j+2, t) - \sum_{k=n-j+1}^{n-i+1} P(k, t+\Delta t \mid n-j+1, t)}{\Delta t}, & i < j \\ 0, & i > j, \end{cases} \tag{13}$$

where λ_{ij} $(1 \le i, j \le n)$ represents the element in the ith row and the jth column of the hazard rate matrix λ.

It is noted that the derivation of Eq. (13) is not dependent on the linear degradation assumption; therefore, the result is general. The significance of Eq. (13) is that it establishes the connection between the elements of the hazard rate matrix and the conditional probabilities. Since the conditional probability describes the instantaneous state variation at time t; therefore, the hazard rate matrix can fully describe the degradation dynamics and vice versa.

3. Reliability model of multi-function systems using hazard rate matrix and Markovian approximation

Consider an n-function system, the reliability functions $\mathbf{R}(t)$ can be expressed as the following by substituting Eq. (8) into Eq. (2)

$$\frac{\mathrm{d}}{\mathrm{d}t}\begin{bmatrix} R_a \\ R_b \\ \vdots \\ R_n \end{bmatrix} = -\begin{bmatrix} \lambda_{aa} & \lambda_{ab} & \cdots & \lambda_{an} \\ 0 & \lambda_{bb} & \cdots & \lambda_{bn} \\ \vdots & \vdots & \ddots & \vdots \\ 0 & 0 & \cdots & \lambda_{nn} \end{bmatrix}\begin{bmatrix} R_a \\ R_b \\ \vdots \\ R_n \end{bmatrix}. \tag{14}$$

Given the initial state $R_i(0) = 1, i \in (a, b, \dots, n)$, Eq. (14) can be solved to obtain

$$\begin{aligned}
R_a &= \exp\left(\int_0^t -\lambda_{aa}\mathrm{d}t'\right)\left\{1 - \int_0^t \left[\lambda_{ab}R_b + \lambda_{ac}R_c + \cdots + \lambda_{an}R_n\right]\right. \\
&\quad \left. \times \exp\left(\int_0^{t'} -\lambda_{aa}\,\mathrm{d}t''\right)\mathrm{d}t'\right\}, \\
&\vdots \\
R_i &= \exp\left(\int_0^t -\lambda_{ii}\mathrm{d}t'\right)\left\{1 - \int_0^t \left[\lambda_{i(i+1)}R_{i+1} + \lambda_{i(i+2)}R_{i+2} + \cdots + \lambda_{in}R_n\right]\right. \\
&\quad \left. \times \exp\left(\int_0^{t'} -\lambda_{ii}\,\mathrm{d}t''\right)\mathrm{d}t'\right\}, \\
&\vdots \\
R_{n-1} &= \exp\left(\int_0^t -\lambda_{(n-1)(n-1)}\mathrm{d}t'\right) \\
&\quad \times \left[1 - \int_0^t \lambda_{(n-1)n}\exp\left(\int_0^{t'} \lambda_{(n-1)(n-1)} - \lambda_{nn}\,\mathrm{d}t''\right)\mathrm{d}t'\right], \\
R_n &= \exp\left(\int_0^t -\lambda_{nn}\mathrm{d}t'\right).
\end{aligned} \tag{15}$$

The joint PDF $p(t_a, t_b, \dots, t_n)$ of the system is difficult to be determined directly due to its complexity. By decomposing the system into the state-function table (e.g., Table 3), the joint PDF of the lifetimes of all functions in an irreducible n-function system can be expressed, by incorporating all the possible failure path from the state-function table, as

$$p\left(t_a, \dots, t_n\right) = \sum_\alpha \mu^\alpha p^\alpha(t_a, \dots, t_n) h(t_a, \dots, t_n), \tag{16}$$

where α represents one possible failure path of all failure paths, μ^α is the probability associated with the failure path α such that $\sum_\alpha \mu^\alpha = 1$, $p^\alpha(t_a, \dots, t_n)$ represents the PDFs of joint lifetimes of all functions $(a, \dots, n)$ when the system fails along the failure path α, and $H(t_a, \dots, t_n)$ is the joint step function constraining the order of failure times of the functions. The actual expression of $H(t_a, \dots, t_n)$ depends on the failure paths of a specific system.

The state transition of a multi-function system describes the dynamical trajectory of the degradation process. The probability for the degradation trajectory $S = (i_0, t_0; i_1, t_1; \cdots; i_m, t_m)$ can be written as the product of conditional probabilities at each time steps as

$$\begin{aligned}
P(S) &= P(i_m, t_m | i_{m-1}, t_{m-1}; \cdots; i_0, t_0) \cdot P(i_{m-1}, t_{m-1}; \cdots; i_0, t_0) \\
&= P(i_m, t_m | i_{m-1}, t_{m-1}; \cdots; i_0, t_0) \\
&\quad \cdot P(i_{m-1}, t_{m-1} | i_{m-2}, t_{m-2}; \cdots; i_0, t_0) \cdot P(i_{m-2}, t_{m-2}; \cdots; i_0, t_0) \\
&= \cdots \\
&= P(i_m, t_m | i_{m-1}, t_{m-1}; \cdots; i_0, t_0) \\
&\quad \cdot P(i_{m-1}, t_{m-1} | i_{m-2}, t_{m-2}; \cdots; i_0, t_0) \cdots P(i_1, t_1 | i_0, t_0) \cdot P(i_0, t_0),
\end{aligned} \tag{17}$$

where the suffix represents the time index. The term $P(i_m, t_m | i_{m-1}, t_{m-1}; \cdots; i_0, t_0)$ is the probability of being in state i_m at time t_m conditional on the system experiencing the previous trajectory $(i_{m-1}, t_{m-1}; \cdots; i_0, t_0)$ in reverse order.

Under Markovian condition, the probability distribution of the future state depends only on the current state. The conditional probability can be simplified as

$$P(i_m, t_m | i_{m-1}, t_{m-1}; \dots; i_0, t_0) = P(i_m, t_m | i_{m-1}, t_{m-1}), \tag{18}$$

for $m \in (1, 2, \dots)$. Furthermore, under this condition, the dynamical equation for the probability $P(j, t)$ of a multi-state system being in state j at time t can be written as

$$\frac{\mathrm{d}P(j,t)}{\mathrm{d}t} = \sum_i k_{ji} P(i, t), \tag{19}$$

where k_{ji} is the transition rate from state i to state j.

One of the key steps in the method is to express the joint PDF of the failure times of all functions in the system using the state transition rates of the whole system. The Markovian approximation is needed to obtain an analytical form of the joint PDF in terms of the state transition rates. In addition, under Markovian condition, the relation between the hazard rate matrix and the state transition rate matrix can also be established. By combining the two results and the dynamical equation of Eq. (19), the equations for the elements in the hazard rate matrix can be established using the observable information on the functions; therefore, the detail of system degradation process can be resolved using the method. Under more general (non-Markovian) conditions, the basic idea of the method remains unchanged; however, the joint PDF of failure times of all functions may not have close-form expressions as the non-Markovian conditions can be varying case-by-case. Consequently, the hazard rate equations do not have close-form expressions, and one has to resort approaches such as Monte Carlo simulations or asymptotic approximations for the required computations, which may be highly nontrivial for multi-function systems. In this case, other methods such as Refs. [44,45] may be used. The overall procedure of the method is demonstrated using the following examples.

Table 4
Four states of an irreducible three-function system.

State	Function a	Function b	Function c
1	Work	Work	Work
2	Work	Work	Breakdown
3	Work	Breakdown	Breakdown
4	Breakdown	Breakdown	Breakdown

4. Engineering applications

An irreducible three-function system is used to illustrate the overall method. The degradation dynamics of the functions is resolved using the proposed method, and the accuracy of the results is verified. The applicability of the method to non-Markovian degradation processes is discussed. Following that, the proposed method is applied to a power system to demonstrate the usage in realistic engineering problems.

4.1. A three-function system demonstration

A three-function system having four different states is used for method demonstration. Without loss of generality, the relation between functions is prescribed as $a \succ b \succ c$, and the resulting four states are shown in Table 4. The hazard rate matrix of this system is

$$\lambda = \begin{bmatrix} \lambda_{aa} & \lambda_{ab} & \lambda_{ac} \\ 0 & \lambda_{bb} & \lambda_{bc} \\ 0 & 0 & \lambda_{cc} \end{bmatrix}. \tag{20}$$

Given the initial condition $R_i(0) = 1$, the solution to the reliability function $R_i(t)$ is obtained using Eq. (15).

The possible failure paths of the system are $\alpha = \{(1234), (134), (124), (14)\}$, according to the states shown in Table 4; consequently, the joint distribution of the failure times of the three functions can be expressed as

$$\begin{aligned}
p\left(t_a, t_b, t_c\right) &= \mu^{(1234)} p^{(1234)}\left(t_a, t_b, t_c\right) h\left(t_a - t_b\right) h\left(t_b - t_c\right) \\
&\quad + \mu^{(134)} p^{(134)}\left(t_a, t_b, t_c\right) h\left(t_a - t_b\right) \delta\left(t_b - t_c\right) \\
&\quad + \mu^{(124)} p^{(124)}\left(t_a, t_b, t_c\right) \delta\left(t_a - t_b\right) h\left(t_b - t_c\right) \\
&\quad + \mu^{(14)} p^{(14)}\left(t_a, t_b, t_c\right) \delta\left(t_a - t_b\right) \delta\left(t_b - t_c\right),
\end{aligned} \tag{21}$$

where $\mu^{(\alpha)}$ is the probability of the failure path α. For example, $\mu^{(1234)}$ represents the probability that the system fails by sequentially experiencing states 1, 2, 3, and 4. The term $p^\alpha\left(t_a, t_b, t_c\right)$ is the joint distribution of failure times of the three functions when the system fails via the path α. For example, $p^{(1234)}(t_a, t_b, t_c)$ is the joint distribution of the failure times of the three functions when the system fails via the failure path (1234). The order of traversing a specific trajectory of states is ensured by the Heaviside function $h(\cdot)$

$$h(x) = \begin{cases} 1 & x > 0 \\ 0 & \text{otherwise,} \end{cases} \tag{22}$$

and the simultaneous failure of two or three functions is ensured by the Dirac delta function $\delta(\cdot)$

$$\delta(x) = \begin{cases} 1 & x = 0 \\ 0 & \text{otherwise.} \end{cases} \tag{23}$$

For a specific function $i \in (a, b, c)$, the marginal PDF of its failure time t can be obtained by integrating out the other variable $j \in (a, b, c), j \neq i$ of Eq. (21) as

$$p_i(t) = \mu^{(1234)} p_i^{(1234)}(t) + \mu^{(134)} p_i^{(134)}(t) + \mu^{(124)} p_i^{(124)}(t) + \mu^{(14)} p_i^{(14)}(t), \tag{24}$$

where $p_i^{\alpha}(t)$ denotes the marginal PDF of the function i's failure time t under the failure path α.

Using Markovian approximation Eq. (18), the joint PDF of failure times of the three functions conditional on a failure path can be derived, For example, the joint probability of the failure times (t_a, t_b, t_c) conditional on the failure path (1234) in a time interval Δt is

$$\begin{aligned}
&\mu^{(1234)} p^{(1234)}(t_a, t_b, t_c) \Delta t^3 \\
=&P(4, t_a; 3, t_a - \Delta t; \cdots; 3, t_b; 2, t_b - \Delta t; \cdots; 2, t_c; 1, t_c - \Delta t; \cdots; 1, 0) \\
=&P(4, t_a | 3, t_a - \Delta t) \\
&\quad \cdot P(3, t_a - \Delta t; \cdots; 3, t_b; 2, t_b - \Delta t; \cdots; 2, t_c; 1, t_c - \Delta t; \cdots; 1, 0) \\
=&P(4, t_a | 3, t_a - \Delta t) \cdot P(3, t_a - \Delta t | 3, t_a - 2\Delta t) \\
&\quad \cdot P(3, t_a - 2\Delta t; \cdots; 3, t_b; \cdots; 2, t_c; \cdots; 1, 0) \\
=&k_{43}(t_a)\Delta t \prod_{j=1}^{n_3} \left[1 + k_{33}(t_a - j\Delta t) \cdot \Delta t\right] \cdot k_{32}(t_b)\Delta t \prod_{j=1}^{n_2} \left[1 + k_{22}(t_b - j\Delta t) \cdot \Delta t\right] \\
&\quad \cdot k_{21}(t_c)\Delta t \prod_{j=1}^{n_1} \left[1 + k_{11}(t_c - j\Delta t) \cdot \Delta t\right],
\end{aligned} \tag{25}$$

where $n_1 = t_c/\Delta t$, $n_2 = (t_b - t_c)/\Delta t$, and $n_3 = (t_a - t_b)/\Delta t$ are the numbers of time steps in states 1,2, and 3, respectively. Note that the last step in Eq. (25) utilizes the infinitesimal definition of the continuous-time Markov chain such that as $\Delta t \to 0^+$, $\forall t > \Delta t$,

$$P(j, t | i, t - \Delta t) = \delta_{ji} + k_{ji}(t)\Delta t + o(\Delta t), \tag{26}$$

where δ_{ji} is the Kronecker delta, i and j are state indicators, k_{ji} is the transition rate from state i to state j, and $o(\Delta t)$ is little-o notation.

Divide both sides of Eq. (25) by Δt^3 to obtain the joint PDF (t_a, t_b, t_c) conditional on the failure path (1234) as Δt approaches zero,

$$\begin{aligned}
\mu^{(1234)} p^{(1234)}(t_a, t_b, t_c) = k_{43}\left(t_a\right) \exp\left(\int_{t_b}^{t_a} k_{33} \mathrm{d}t\right) \cdot k_{32}\left(t_b\right) \\
\times \exp\left(\int_{t_c}^{t_b} k_{22} \mathrm{d}t\right) \cdot k_{21}\left(t_c\right) \exp\left(\int_0^{t_c} k_{11} \mathrm{d}t\right).
\end{aligned} \tag{27}$$

Similarly, the joint PDFs of (t_a, t_b, t_c) conditional on all other failure paths can be obtained as,

$$\begin{aligned}
\mu^{(1234)} p^{(1234)}(t_a, t_b, t_c) &= k_{43}(t_a) \exp\left(\int_{t_b}^{t_a} k_{33} \mathrm{d}t\right) \cdot k_{32}(t_b) \\
&\quad \times \exp\left(\int_{t_c}^{t_b} k_{22} \mathrm{d}t\right) \cdot k_{21}(t_c) \exp\left(\int_0^{t_c} k_{11} \mathrm{d}t\right) \\
\mu^{(134)} p^{(134)}(t_a, t_b, t_c) &= k_{43}(t_a) \exp\left(\int_{t_{bc}}^{t_a} k_{33} \mathrm{d}t\right) \cdot k_{31}(t_{bc}) \\
&\quad \exp\left(\int_0^{t_{bc}} k_{11} \mathrm{d}t\right) \\
\mu^{(124)} p^{(124)}(t_a, t_b, t_c) &= k_{42}(t_{ab}) \exp\left(\int_{t_c}^{t_{ab}} k_{22} \mathrm{d}t\right) \cdot k_{21}(t_c) \\
&\quad \exp\left(\int_0^{t_c} k_{11} \mathrm{d}t\right) \\
\mu^{(14)} p^{(14)}(t_a, t_b, t_c) &= k_{41}(t_{abc}) \exp\left(\int_0^{t_{abc}} k_{11} \mathrm{d}t\right).
\end{aligned} \tag{28}$$

In Eq. (28), the term t_{bc} on the right hand side of $\mu^{(134)} p^{(134)}(t_a, t_b, t_c)$ denotes the time when functions b and c simultaneously fail. In the same manner, the term t_{ab} is the simultaneous failure time of functions a and b, and the term t_{abc} is the simultaneous failure time of the three functions a, b, and c.

On the other hand, the relation between the hazard rate matrix λ and the transition rate matrix $\boldsymbol{k}$ can be established, with the detailed derivation presented in Appendix A, as

$$\begin{aligned}
\lambda &= \begin{bmatrix} \lambda_{aa} & \lambda_{ab} & \lambda_{ac} \\ 0 & \lambda_{bb} & \lambda_{bc} \\ 0 & 0 & \lambda_{cc} \end{bmatrix} \\
&= -\begin{bmatrix} -k_{43} & -k_{42} + k_{43} & -k_{41} + k_{42} \\ 0 & -k_{32} - k_{42} & k_{32} + k_{42} - k_{31} - k_{41} \\ 0 & 0 & -k_{21} - k_{31} - k_{41} \end{bmatrix}.
\end{aligned} \tag{29}$$

For the three-function system, the failure rate equations are obtained by combining Eqs. (15), (28), and (29) as

$$\begin{aligned}
&\dot{\lambda}_{aa} - \lambda_{aa}^2 \frac{\mu^{(1234)} p_a^{(1234)} + \mu^{(134)} p_a^{(134)} - \mu^{(1234)} p_b^{(1234)} - \mu^{(134)} p_b^{(134)}}{\mu^{(1234)} p_a^{(1234)} + \mu^{(134)} p_a^{(134)}} \\
&\quad - \lambda_{aa} \frac{\mathrm{d} \ln\left(\mu^{(1234)} p_a^{(1234)} + \mu^{(134)} p_a^{(134)}\right)}{\mathrm{d}t} = 0, \\
&\lambda_{ab} = \frac{\mu^{(124)} p_a^{(124)}}{R_b - R_c} - \lambda_{aa}, \\
&\lambda_{ac} = \frac{\mu^{(14)} p_a^{(14)}}{R_c} - \frac{\mu^{(124)} p_a^{(124)}}{R_b - R_c}, \\
&\dot{\lambda}_{bb} - \lambda_{bb}^2 \left[\frac{\mu^{(1234)} p_b^{(1234)} + \mu^{(124)} p_b^{(124)} - \mu^{(1234)} p_c^{(1234)} - \mu^{(124)} p_c^{(124)}}{\mu^{(1234)} p_b^{(1234)} + \mu^{(124)} p_b^{(124)}}\right] \\
&\quad - \lambda_{bb} \frac{\mathrm{d} \ln\left(\mu^{(1234)} p_b^{(1234)} + \mu^{(124)} p_b^{(124)}\right)}{\mathrm{d}t} = 0, \\
&\lambda_{bc} = \frac{\mu^{(14)} p_b^{(14)} + \mu^{(134)} p_b^{(134)}}{R_c} - \lambda_{bb}, \\
&\dot{\lambda}_{cc} - \lambda_{cc}^2 - \lambda_{cc} \frac{\mathrm{d} \ln p_c}{\mathrm{d}t} = 0,
\end{aligned} \tag{30}$$

where p_c is given by Eq. (24).

The solution to the above system of equations is

$$\begin{aligned}
\lambda_{aa} &= -\frac{\mu^{(1234)}p_a^{(1234)} + \mu^{(134)}p_a^{(134)}}{\int_0^t \left[\mu^{(1234)}p_a^{(1234)} + \mu^{(134)}p_a^{(134)} - \mu^{(1234)}p_b^{(1234)} - \mu^{(134)}p_b^{(134)}\right] \mathrm{d}t'},\\
\lambda_{ab} &= \frac{\mu^{(124)}p_a^{(124)}}{R_b - R_c} - \lambda_{aa},\\
\lambda_{ac} &= \frac{\mu^{(14)}p_a^{(14)}}{R_c} - \frac{\mu^{(124)}p_a^{(124)}}{R_b - R_c},\\
\lambda_{bb} &= -\frac{\mu^{(1234)}p_b^{(1234)} + \mu^{(124)}p_b^{(124)}}{\int_0^t \left[\mu^{(1234)}p_b^{(1234)} + \mu^{(124)}p_b^{(124)} - \mu^{(1234)}p_c^{(1234)} - \mu^{(124)}p_c^{(124)}\right] \mathrm{d}t'},\\
\lambda_{bc} &= \frac{\mu^{(14)}p_b^{(14)} + \mu^{(134)}p_b^{(134)}}{R_c} - \lambda_{bb},\\
\lambda_{cc} &= \frac{p_c}{1 - \int_0^t p_c \, \mathrm{d}t'}.
\end{aligned} \tag{31}$$

Eq. (31) provides an explicit relation between the marginal PDFs (such as $p_a^{(1234)}$, $p_a^{(134)}$, etc.) and the elements of the hazard rate matrix under Markovian condition. With this result, the details of system degradation process can be inferred with the information (such as lifetime data) on the functions. It should be noted that the method itself does not depend on the failure information nor the means obtaining such information to formulate the equations and obtain their symbolic solutions; however, the equations can only be numerically resolved with the actual failure time information on these functions. In realistic cases such information can be assumed, calculated from physics-based models, and/or obtained from testing data.

To demonstrate the computation, the transition rate matrix $\boldsymbol{k}$ in Eq. (32) is assumed. Substitute the terms in Eq. (32) into Eq. (28) to obtain the required marginal PDFs on the right hand side of Eq. (31), representing the observed marginal PDFs. The elements of the hazard rate matrix are evaluated and the results are shown as solid lines in Fig. 1. Note that the results represent the solution to the hazard rate matrix of the three-function system obtained using observable information on the functions.

$$\boldsymbol{k} = \begin{bmatrix} \mathrm{e}^{-5t}-1 & 0 & 0 & 0 \\ \mathrm{e}^{-4t}-\mathrm{e}^{-5t} & \mathrm{e}^{-3t}-1 & 0 & 0 \\ \mathrm{e}^{-3t}-\mathrm{e}^{-4t} & \mathrm{e}^{-2t}-\mathrm{e}^{-3t} & \mathrm{e}^{-t}-1 & 0 \\ 1-\mathrm{e}^{-3t} & 1-\mathrm{e}^{-2t} & 1-\mathrm{e}^{-t} & 0 \end{bmatrix}. \tag{32}$$

To verify the accuracy of Eq. (31), the hazard rate matrix can directly be calculated using the assumed transition rate matrix Eq. (32) according to Eq. (29). The direct results represent ground truth values, and are presented as discrete markers in Fig. 1. By comparing the two sets of results, a close agreement between the two is observed, indicating that the result of Eq. (31) is accurate.

It is worth mentioning that in realistic cases, the transition rate matrix is rarely known a priori, and only failure time data are available on certain functions; however, the actual solution to the hazard rate matrix of the system, such as Eq. (31), can be resolved using the proposed method. As shown in Eq. (31), only marginal PDFs such as $p_a^{(1234)}$, $p_b^{(134)}$, and so on are needed. Those marginal PDFs can be obtained using proper probabilistic and/or statistical methods and lifetime data on the functions. Furthermore, it should be stressed that the equations of the elements of the hazard rate matrix, e.g., Eq. (30) and the solutions to the equations, e.g., Eq. (31) are only analytically tractable under Markovian condition. For non-Markovian conditions, the performance of the method depends on the memory time of the specific non-Markovian process which can be different case-by-case. A detailed error analysis using the three-function system example is presented in Appendix B. It is shown that, by using Markovian approximation to a non-Markovian process, the error grows as the memory time increases, and the error does not exceed 20% in this example.

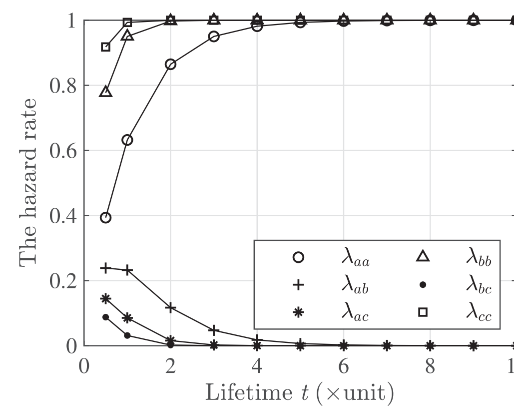

Fig. 1. The comparison between the actual (in discrete markers) and solved (in solid lines) elements of the hazard rate matrix.

Table 5
States and functions of the power system.

State	Function c_1	Function c_2	Function b_2	Function a
1	Work	Work	Work	Work
2	Breakdown	Work	Work	Breakdown
3	Work	Breakdown	Work	Breakdown
4	Work	Work	Breakdown	Breakdown
5	All other states			

4.2. A power system reliability assessment problem

A power system reliability assessment problem is adopted to demonstrate the method in realistic engineering applications. The power system model is taken from Ref. [46] where the actual system is modeled using the fault tree analysis, and the simplified fault tree model is shown in Fig. 2 for demonstration purposes. The function a represents the substation works, and functions b_1 and b_2 represent the electricity transfer works properly for generator/load and lines, respectively. Function b_1 can be divided into two functions c_1 and c_2, which represent the electricity transfer paths from generators to lines, and from lines to loads are in working state, respectively. It is noted that the state of function b_1 can be determined by the states of c_1 and c_2, and the functions a, b_2, c_1 and c_2 determine the state of the whole system. A total of five states are possible for the system and are shown in Table 5. Since the probability of the event that multiple functions fail simultaneously is almost zero in actual engineering, the possible failure paths of the system reduce to one of the three in the set $\alpha = \{(125), (135), (145)\}$, where the numbers in $(\cdot)$ denotes the system fails via the sequence of states indexed by the numbers, as defined before.

Following the procedure outlined in Section 2, the hazard rate matrix of the power system is expressed as

$$\lambda = \begin{bmatrix} \lambda_{c_1c_1} & 0 & 0 & \lambda_{c_1a} \\ 0 & \lambda_{c_2c_2} & 0 & \lambda_{c_2a} \\ 0 & 0 & \lambda_{b_2b_2} & \lambda_{b_2a} \\ 0 & 0 & 0 & \lambda_{aa} \end{bmatrix}. \tag{33}$$

Referring to the procedure in Appendix A, the relationship between the hazard rate matrix and transition rate matrix of the system is established as Eq. (34) given in Box I.

The equations for the elements in the hazard rate matrix of the system are formulated following the procedure described in Section 3.

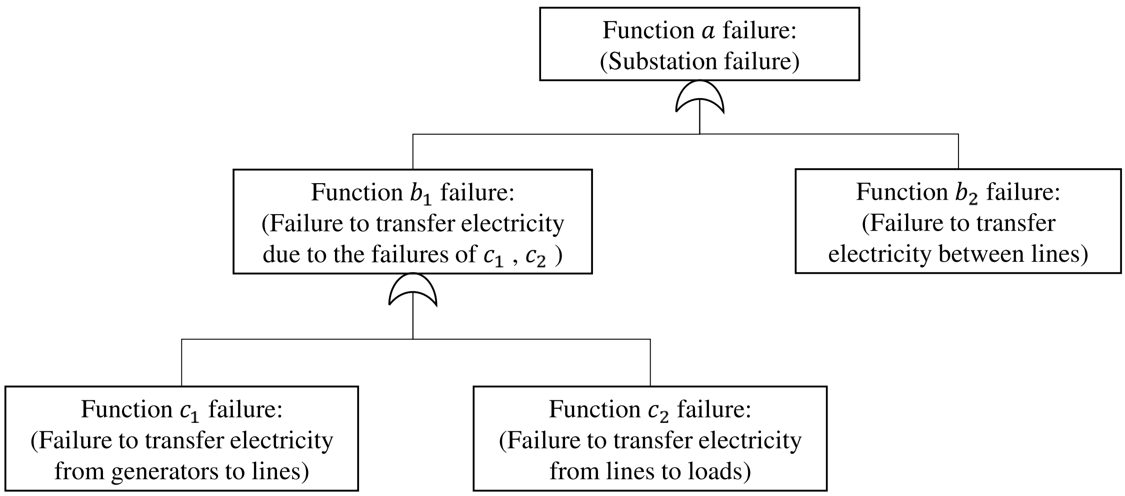

Fig. 2. Fault tree diagram of the power system.

$$
\boldsymbol{k}^T = \begin{bmatrix} k_{11} & k_{21} & k_{31} & k_{41} & k_{51} \\ k_{12} & k_{22} & k_{32} & k_{42} & k_{52} \\ k_{13} & k_{23} & k_{33} & k_{43} & k_{53} \\ k_{14} & k_{24} & k_{34} & k_{44} & k_{54} \\ k_{15} & k_{25} & k_{35} & k_{45} & k_{55} \end{bmatrix}
= \begin{bmatrix} -\lambda_{aa} & \lambda_{c_1 a} + \lambda_{c_1 c_1} & \lambda_{c_2 a} + \lambda_{c_2 c_2} & \lambda_{b_2 a} + \lambda_{b_2 b_2} & 0 \\ 0 & \lambda_{c_1 c_1} - \lambda_{c_2 c_2} - \lambda_{b_2 b_2} & 0 & 0 & \lambda_{c_2 c_2} + \lambda_{b_2 b_2} - \lambda_{c_1 c_1} \\ 0 & 0 & \lambda_{c_2 c_2} - \lambda_{c_1 c_1} - \lambda_{b_2 b_2} & 0 & \lambda_{c_1 c_1} + \lambda_{b_2 b_2} - \lambda_{c_2 c_2} \\ 0 & 0 & 0 & \lambda_{b_2 b_2} - \lambda_{c_1 c_1} - \lambda_{c_2 c_2} & \lambda_{c_1 c_1} + \lambda_{c_2 c_2} - \lambda_{b_2 b_2} \\ 0 & 0 & 0 & 0 & 0 \end{bmatrix} \quad (34)
$$

Box I.

The solutions to the equations are

$$
\begin{aligned}
\lambda_{c_1 c_1} &= -\frac{p_{c_1} - \mu^{(125)} p_{c_1}^{(125)}}{\int_0^t (p_{c_1} - p_a)\, \mathrm{d}t'}, \\
\lambda_{c_1 a} &= \frac{\mu^{(125)} p_{c_1}^{(125)}}{1 - \int_0^t p_a\, \mathrm{d}t'} + \frac{p_{c_1} - \mu^{(125)} p_{c_1}^{(125)}}{\int_0^t (p_{c_1} - p_a)\, \mathrm{d}t'}, \\
\lambda_{c_2 c_2} &= -\frac{p_{c_2} - \mu^{(135)} p_{c_2}^{(135)}}{\int_0^t (p_{c_2} - p_a)\, \mathrm{d}t'}, \\
\lambda_{c_2 a} &= \frac{\mu^{(135)} p_{c_2}^{(135)}}{1 - \int_0^t p_a\, \mathrm{d}t'} + \frac{p_{c_2} - \mu^{(135)} p_{c_2}^{(135)}}{\int_0^t (p_{c_2} - p_a)\, \mathrm{d}t'}, \\
\lambda_{b_2 b_2} &= -\frac{p_{b_2} - \mu^{(145)} p_{b_2}^{(145)}}{\int_0^t (p_{b_2} - p_a)\, \mathrm{d}t'}, \\
\lambda_{b_2 a} &= \frac{\mu^{(145)} p_{b_2}^{(145)}}{1 - \int_0^t p_a\, \mathrm{d}t'} + \frac{p_{b_2} - \mu^{(145)} p_{b_2}^{(145)}}{\int_0^t (p_{b_2} - p_a)\, \mathrm{d}t'}, \\
\lambda_{aa} &= \frac{p_a}{1 - \int_0^t p_a\, \mathrm{d}t'} = \frac{\mu^{(125)} p_a^{(125)} + \mu^{(135)} p_a^{(135)} + \mu^{(145)} p_a^{(145)}}{1 - \int_0^t \left[\mu^{(125)} p_a^{(125)} + \mu^{(135)} p_a^{(135)} + \mu^{(145)} p_a^{(145)}\right] \mathrm{d}t'},
\end{aligned} \quad (35)
$$

where p_i^α, $i \in (a, b_2, c_1, c_2)$ is defined as before, representing the marginal distribution of function i's failure time when the system degrades along the path α. The total marginal distribution for function i is $p_i = \sum_\alpha \mu^\alpha p_i^\alpha$, and μ^α is the probability that the system degrades along the path α.

To demonstrate the results, the probabilities of failure paths are arbitrarily set as $\mu^{(125)} = 0.5$, $\mu^{(135)} = 0.2$ and $\mu^{(145)} = 0.3$. Furthermore, assume the observed failure times of the functions follow Weibull distributions. Specifically, it is assumed that the first function has a failure time PDF of $p_i^\alpha(t) = 2t\mathrm{e}^{-t^2}$ and all other functions have a failure time PDF of $p_i^\alpha(t) = t\mathrm{e}^{-0.5t^2}$. For example, for $\alpha = (125)$, $p_{c_1}^{(125)} = 2t\mathrm{e}^{-t^2}$ and $p_{c_2}^{(125)} = p_{b_2}^{(125)} = p_a^{(125)} = t\mathrm{e}^{-0.5t^2}$. With the failure time PDFs, the elements of the hazard rate matrix can be resolved using Eq. (35). Furthermore, the probabilities of states $P_j, j = (1, \ldots, 5)$ can be obtained by solving the system of differential equations Eq. (19) using the transition rate matrix of Eq. (34). The results are shown in Fig. 3. In particular, the curve labeled as 'State 1' is the time-dependent reliability of the system (i.e., the probability of the system being in State 1). For example, given a rated lifetime of $t = 0.5$ (×unit), the reliability of the power system is 0.7788, and the failure probabilities of function a caused by functions c_1, c_2, and b_2 are 0.0518, 0.0207 and 0.0311, respectively.

Note that the observable information in this case is simulated using the assumed failure time PDFs of the individual functions; therefore, the verification of the accuracy of the results shown in Fig. 3 can be made following the procedure described in Section 4.1, and is omitted here due to redundancy. In actual cases, the failure time PDFs can be obtained using proper probabilistic and/or statistical methods and failure information on the functions, such as lifetime data.

5. Conclusion

A new method to model the degradation and reliability of complex systems was developed in this study. The basic idea of the proposed

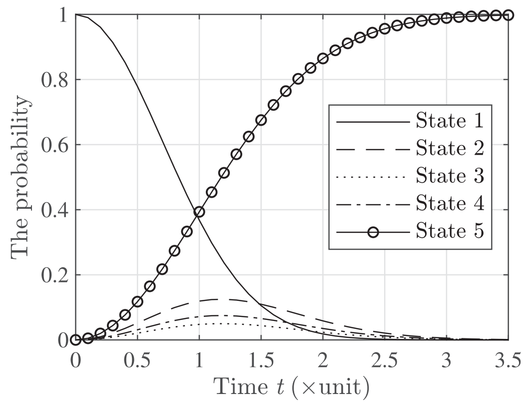

Fig. 3. The probabilities of the state of the system at different times.

method is to abstract a system as a set of states which are determined by the functions of the system. The hazard rate matrix is proposed to describe the degradation of the functions. A diagonal term in the hazard rate matrix describes the degradation of a particular function and a non-diagonal term describes the degradation contributed by other influencing functions. By incorporating the Markovian approximation, the equations for each of the elements in the hazard rate matrix can be formulated, and subsequently be solved using failure information on the functions. In this sense the method is applicable to general complex systems. An example was used to illustrate the overall procedure of the method, and the accuracy of the results was verified. A power system reliability assessment problem is provided to demonstrate its applicability in realistic engineering problems. Based on the current results, the following conclusions are drawn.

(1) The proposed hazard rate matrix provides a general mathematical tool to characterize the degradation of the system based on its functions, and the correlations among these functions are naturally dealt with by the non-diagonal terms of the matrix without special treatments.
(2) The relationship between the hazard rate matrix and the transition rate matrix can be established for a general multi-function system under the Markovian condition. Close-form expressions for the equations of the elements in the hazard rate matrix and their solutions can be obtained under this condition.

As the method is centered on the state-based modeling, it predicts the faults and remaining useful life of the system in terms of states, e.g., healthy or faulty. However, it in general cannot predict the faults of an individual component except that the component individually corresponds to a function of the system. It should be noted that the developed method can yield close-form expressions of the hazard rate equations and their solutions only under the Markovian condition. For more general non-Markovian conditions, the method can still be applied but no close-form equations and their solutions are available. In these cases, other evaluation techniques, such as Monte Carlo simulations or asymptotic approximations, can be used for the computation. The use of Markovian approximation to a non-Markovian process can yield modeling error, as demonstrated in this study. In addition, the method relies on the failure information on the functions to obtain numeric results. When no such information is available, the method can still be applied to obtain symbolic results, but no quantitative (numeric) results can be realized.

CRediT authorship contribution statement

Daoqing Zhou: Methodology, Computational code development, Original draft preparation, Revision. **C.P. Sun:** Review. **Yi-Mu Du:** Methodology. **Xuefei Guan:** Conceptualization, Methodology, Review, Revision.

Declaration of competing interest

The authors declare that they have no known competing financial interests or personal relationships that could have appeared to influence the work reported in this paper.

Acknowledgments

The study was supported by National Natural Science Foundation of China, Nos. 51975546, 12088101, U1930403 and by CAEP, China CX20200035. The support is gratefully acknowledged. Authors would like to thank the anonymous reviewers for their constructive comments.

Appendix A. The relationship between the hazard rate matrix and Markovian transition rate matrix

According to Table 4, the change between the four states can be described using Eq. (19) as

$$\frac{\mathrm{d}}{\mathrm{d}t}\begin{bmatrix} P_1 \\ P_2 \\ P_3 \\ P_4 \end{bmatrix} = \begin{bmatrix} k_{11} & k_{12} & k_{13} & k_{14} \\ k_{21} & k_{22} & k_{23} & k_{24} \\ k_{31} & k_{32} & k_{33} & k_{34} \\ k_{41} & k_{42} & k_{43} & k_{44} \end{bmatrix}\begin{bmatrix} P_1 \\ P_2 \\ P_3 \\ P_4 \end{bmatrix}, \tag{A.1}$$

where $P_j, j \in (1, \ldots, 4)$ is the probability when the system is in the state j at time t, and k_{ji} is the transition rate from state i to state j. Due to the absence of system recovery, $k_{ji} = 0$ $(\forall i > j)$. From Table 4,

$$\begin{cases} R_a = P_1 + P_2 + P_3 \\ R_b = P_1 + P_2 \\ R_c = P_1. \end{cases} \tag{A.2}$$

Differentiate both sides of Eq. (A.2) with respect to t, and substitute Eq. (A.1) into the resulting derivatives to have

$$\frac{\mathrm{d}}{\mathrm{d}t}\begin{bmatrix} R_a \\ R_b \\ R_c \end{bmatrix} = \begin{bmatrix} k_{33} & k_{22}+k_{32}-k_{33} & k_{11}+k_{21}+k_{31}-k_{22}-k_{32} \\ 0 & k_{22} & k_{11}+k_{21}-k_{22} \\ 0 & 0 & k_{11} \end{bmatrix}\begin{bmatrix} R_a \\ R_b \\ R_c \end{bmatrix}. \tag{A.3}$$

The total probability of all the possible states is unity, i.e.,

$$\sum_j P_j = 1. \tag{A.4}$$

Therefore,

$$\frac{\mathrm{d}\left[\sum_j P_j\right]}{\mathrm{d}t} = \sum_j \left[\frac{\mathrm{d}P_j}{\mathrm{d}t}\right] = 0. \tag{A.5}$$

The term $\mathrm{d}P_j/\mathrm{d}t = \sum_i k_{ji}P_i$ according to Eq. (19). Substitute the term into Eq. (A.5) to obtain

$$\begin{aligned}\sum_j \sum_i k_{ji}P_i &= (k_{11}+k_{21}+k_{31}+k_{41})P_1 + (k_{12}+k_{22}+k_{32}+k_{42})P_2 \\ &\quad + (k_{13}+k_{23}+k_{33}+k_{43})P_3 + (k_{14}+k_{24}+k_{34}+k_{44})P_4 \\ &= 0 \end{aligned} \tag{A.6}$$

The probabilities $P_i, i \in (1, \ldots, 4)$ are non-negative by definition. For nontrivial solutions to Eq. (A.6), i.e., $P_i \neq 0, i \in (1, \ldots, 4)$, it requires

$$\sum_j k_{ji} = 0 \; (i, j = 1, 2, 3, 4) \tag{A.7}$$

Using Eq. (A.7) and $k_{ji} = 0$ $(\forall i > j)$, Eq. (A.3) can be rewritten as

$$\frac{\mathrm{d}}{\mathrm{d}t}\begin{bmatrix} R_a \\ R_b \\ R_c \end{bmatrix} = \begin{bmatrix} -k_{43} & -k_{42}+k_{43} & -k_{41}+k_{42} \\ 0 & -k_{32}-k_{42} & k_{32}+k_{42}-k_{31}-k_{41} \\ 0 & 0 & -k_{21}-k_{31}-k_{41} \end{bmatrix}\begin{bmatrix} R_a \\ R_b \\ R_c \end{bmatrix}. \tag{A.8}$$

The reliabilities of the functions a, b, and c in the three-function system can be expressed, according to Eq. (14), as

$$\frac{\mathrm{d}}{\mathrm{d}t}\begin{bmatrix} R_a \\ R_b \\ R_c \end{bmatrix} = -\begin{bmatrix} \lambda_{aa} & \lambda_{ab} & \lambda_{ac} \\ 0 & \lambda_{bb} & \lambda_{bc} \\ 0 & 0 & \lambda_{cc} \end{bmatrix}\begin{bmatrix} R_a \\ R_b \\ R_c \end{bmatrix}. \tag{A.9}$$

Compare Eq. (A.8) with Eq. (A.9), the following element-wise relationship between the hazard rate matrix and the transition rate matrix is established,

$$\lambda = \begin{bmatrix} \lambda_{aa} & \lambda_{ab} & \lambda_{ac} \\ 0 & \lambda_{bb} & \lambda_{bc} \\ 0 & 0 & \lambda_{cc} \end{bmatrix} = -\begin{bmatrix} -k_{43} & -k_{42}+k_{43} & -k_{41}+k_{42} \\ 0 & -k_{32}-k_{42} & k_{32}+k_{42}-k_{31}-k_{41} \\ 0 & 0 & -k_{21}-k_{31}-k_{41} \end{bmatrix}. \tag{A.10}$$

Appendix B. Error analysis for a non-Markovian process

The Markovian approximation is used to model the actual dynamical process of a multi-function system which can be Markovian or non-Markovian. From the perspective of modeling, it is a simplification of the actual process whose property (Markovian or non-Markovian) in general is not known a priori. In other words, if the property of a process is known, the Markovian assumption would not be needed at the first place. In this sense, the Markovian assumption is a choice on the modeling treatment; consequently, it can be verified by comparing the results obtained using the Markovian approximation and that alternatively obtained without using the assumption. If these two sets of results show no significant deviation, using Markovian assumption can loosely be justified.

For a non-Markovian process, the state at time t is affected by the historical states. Consider a non-Markovian process trajectory $S = (i_0, t_0; i_1, t_1; \cdots; i_m, t_m)$ in which the current state is affected by a time length τ, i.e., memory time. For the purpose of simulating a non-Markovian process, the current transition rate is determined using the time window average, and is calculated as

$$k_{j[S]} = \frac{1}{\tau}\left[k_{j[S(t)]} + k_{j[S(t-1)]} + k_{j[S(t-2)]} + \cdots + k_{j[S(t-\tau)]}\right], \tag{B.1}$$

where $k_{j[S]}$ is the transition rate from the current trajectory S to next state j, $S(\cdot)$ is the actual state indexed by $\cdot$, and $\mathcal{S}$ is the state space of the trajectory S. Denote the probability of the trajectory S as P_S, the dynamical equation of the probability P_j is

$$\frac{\mathrm{d}P_j}{\mathrm{d}t} = \sum_{S\in\mathcal{S}} k_{j[S]} P_S. \tag{B.2}$$

Note that Eq. (B.1) is arbitrarily chosen to represent a non-Markovian process. Other conditions that can substantiate a non-Markovian process can also be used.

The three-function system presented in Section 4.1 is used as the system under modeling. To demonstrate the performance of the proposed method in solving a non-Markovian process, the following transition rate matrix is used for simplicity

$$\boldsymbol{k}^T = \begin{bmatrix} -0.9 & 0.6 & 0.2 & 0.1 \\ 0 & -0.5 & 0.3 & 0.1 \\ 0 & 0 & -0.2 & 0.2 \\ 0 & 0 & 0 & 0 \end{bmatrix}, \tag{B.3}$$

and the effect of the memory time τ is studied.

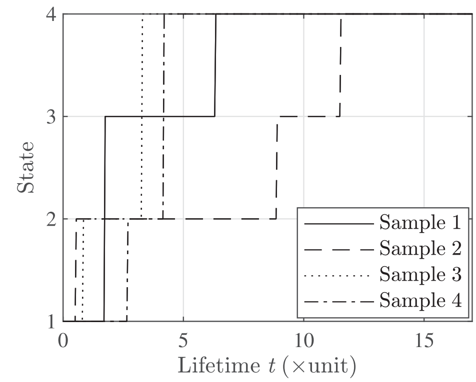

Fig. B.4. Four arbitrarily chosen samples of the state trajectory.

Table B.6
The memory time τ and the resulting error ε.

τ	0.05	0.1	0.25	0.5	1	3	5	8	10
ε	0.1374	0.1380	0.1432	0.1484	0.1542	0.1584	0.1588	0.1591	0.1594

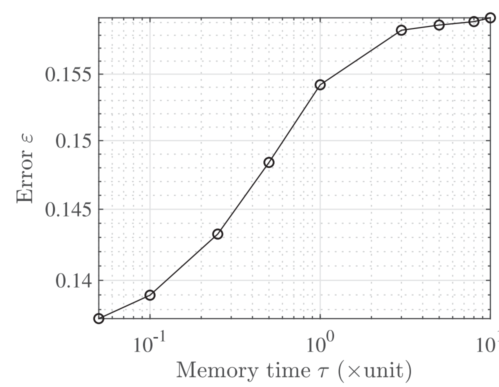

Fig. B.5. The error ε vs. the memory time τ.

Given the memory time τ, the non-Markovian process can be simulated. In this example, a total number of 10^8 trajectories are generated. Fig. B.4 shows four simulated trajectories for illustration. Due to the high computational demand, for each of the trajectories, a total length of 50 time steps are simulated with a time interval of $\Delta t = 0.05$. The joint PDF can be statistically determined using the resulting trajectory samples, which is expressed as $p(t_a, t_b, t_c)$ and is considered as the ground truth.

The marginal PDFs are obtained from the resulting trajectory samples to represent the observable information. The derived joint PDF, labeled as $p_*(t_a, t_b, t_c)$, is obtained by Eq. (31). The Kolmogorov distance [47] is employed to quantify the error ε between the $p(t_a, t_b, t_c)$ and $p_*(t_a, t_b, t_c)$,

$$\varepsilon = \int \frac{1}{2}\left|p(t_a, t_b, t_c) - p_*(t_a, t_b, t_c)\right| \mathrm{d}t_a \mathrm{d}t_b \mathrm{d}t_c. \tag{B.4}$$

The errors ε under different memory time lengths τ are evaluated using the above procedure, and results are shown in Table B.6 and Fig. B.5. It is shown that the error ε grows as the memory time τ increases. The resulting error is less than 20% in the current range of τ.

References

[1] NASA CR-1129: Reliability prediction vol. IV - prediction. Tech. rep., Research Triangle Institute, Research Triangle Park, NC; 1968.

[2] Davis D. An analysis of some failure data. J Amer Statist Assoc 1952;47(258):113–50.
[3] Levenbach G. Accelerated life testing of capacitors. IRE Trans Reliab Qual Control 1957;9–20.
[4] Krohn CA. Hazard versus renewal rate of electronic items. IEEE Trans Reliab 1969;18(2):64–73.
[5] Lux W. A reliability study of diesel engines. Tech. rep., SAE Technical Paper; 1964.
[6] Klutke GA, Kiessler PC, Wortman MA. A critical look at the bathtub curve. IEEE Trans Reliab 2003;52(1):125–9.
[7] Pham H, Lai CD. On recent generalizations of the Weibull distribution. IEEE Trans Reliab 2007;56(3):454–8.
[8] Kang WH, Song J, Gardoni P. Matrix-based system reliability method and applications to bridge networks. Reliab Eng Syst Saf 2008;93(11):1584–93.
[9] Choe DE, Gardoni P, Rosowsky D, Haukaas T. Probabilistic capacity models and seismic fragility estimates for RC columns subject to corrosion. Reliab Eng Syst Saf 2008;93(3):383–93.
[10] Kelly DL, Smith CL. Bayesian inference in probabilistic risk assessment—the current state of the art. Reliab Eng Syst Saf 2009;94(2):628–43.
[11] Guan X, Jha R, Liu Y. Model selection, updating, and averaging for probabilistic fatigue damage prognosis. Struct Saf 2011;33(3):242–9.
[12] Huo H, He J, Guan X. A Bayesian fusion method for composite damage identification using Lamb wave. Struct Health Monit 2020;1475921720945000.
[13] Nguyen H, Gouno E. Bayesian inference for common cause failure rate based on causal inference with missing data. Reliab Eng Syst Saf 2020;197:106789.
[14] Jaynes ET. Information theory and statistical mechanics. Phys Rev 1957;106(4):620.
[15] Jaynes ET. On the rationale of maximum-entropy methods. Proc IEEE 1982;70(9):939–52.
[16] Zhou D, He J, Du Y, Sun C, Guan X. Probabilistic information fusion with point, moment and interval data in reliability assessment. Reliab Eng Syst Saf 2021;107790.
[17] Carey MB, Koenig RH. Reliability assessment based on accelerated degradation: A case study. IEEE Trans Reliab 1991;40(5):499–506.
[18] Meeker WQ, LuValle MJ. An accelerated life test model based on reliability kinetics. Technometrics 1995;37(2):133–46.
[19] He J, Chen J, Guan X. Lifetime distribution selection for complete and censored multi-level testing data and its influence on probability of failure estimates. Struct Multidiscip Optim 2020;62(1):1–17.
[20] Boudali H, Dugan JB. A discrete-time Bayesian network reliability modeling and analysis framework. Reliab Eng Syst Saf 2005;87(3):337–49.
[21] Weber P, Jouffe L. Complex system reliability modelling with dynamic object oriented Bayesian networks (DOOBN). Reliab Eng Syst Saf 2006;91(2):149–62.
[22] Mi J, Li YF, Peng W, Huang HZ. Reliability analysis of complex multi-state system with common cause failure based on evidential networks. Reliab Eng Syst Saf 2018;174:71–81.
[23] Lisnianski A. Extended block diagram method for a multi-state system reliability assessment. Reliab Eng Syst Saf 2007;92(12):1601–7.
[24] Guo H, Yang X. A simple reliability block diagram method for safety integrity verification. Reliab Eng Syst Saf 2007;92(9):1267–73.
[25] Lee D, Pan R. Predictive maintenance of complex system with multi-level reliability structure. Int J Prod Res 2017;55(16):4785–801.
[26] Willenborg J, Engle R, Wood H. A crack growth retardation model using an effective stress concept. Tech. rep., Air Force Flight Dynamics Lab Wright-Patterson Afb Oh; 1971.
[27] Schijve J, Skorupa M, Skorupa A, Machniewicz T, Gruszczynski P. Fatigue crack growth in the aluminium alloy D16 under constant and variable amplitude loading. Int J Fatigue 2004;26(1):1–15.
[28] Wang X, Zhao Y, Wang L, Wei L, He J, Guan X. In-situ SEM investigation and modeling of small crack growth behavior of additively manufactured titanium alloy. Int J Fatigue 2021;149:106303.
[29] Duan X, Yuan H, Tang W, He J, Guan X. A general temperature-dependent stress–strain constitutive model for polymer-bonded composite materials. Polymers 2021;13(9):1393.
[30] Duan X, Yuan H, Tang W, He J, Guan X. A phenomenological primary–secondary–tertiary creep model for polymer-bonded composite materials. Polymers 2021;13(14):2353.
[31] Rudra B, Jennings D. Failure-mechanism models for conductive-filament formation. IEEE Trans Reliab 1994;43(3):354–60.
[32] Waldmann T, Gorse S, Samtleben T, Schneider G, Knoblauch V, Wohlfahrt Mehrens M. A mechanical aging mechanism in lithium-ion batteries. J Electrochem Soc 2014;161(10):A1742.
[33] Liao H. Degradation models and design of accelerated degradation testing plans. Rutgers The State University of New Jersey-New Brunswick; 2004.
[34] Gorjian N, Ma L, Mittinty M, Yarlagadda P, Sun Y. A review on degradation models in reliability analysis. In: Engineering asset lifecycle management. Springer; 2010, p. 369–84.
[35] He J, Huo H, Guan X, Yang J. A Lamb wave quantification model for inclined cracks with experimental validation. Chin J Aeronaut 2021;34(2):601–11.
[36] He J, Huang M, Wang W, Wang S, Guan X. An asymptotic stochastic response surface approach to reliability assessment under multi-source heterogeneous uncertainties. Reliab Eng Syst Saf 2021;107804.
[37] Gao C, Fang Z, Lin J, Guan X, He J. Model averaging and probability of detection estimation under hierarchical uncertainties for Lamb wave detection. Mech Syst Signal Process 2022;165:108302.
[38] Du Y, Ma Y, Wei Y, Guan X, Sun C. Maximum entropy approach to reliability. Phys Rev E 2020;101(1):012106.
[39] Du YM, Chen JF, Guan X, Sun C. Maximum entropy approach to reliability of multi-component systems with non-repairable or repairable components. Entropy 2021;23(3):348.
[40] Jia G, Gardoni P. State-dependent stochastic models: A general stochastic framework for modeling deteriorating engineering systems considering multiple deterioration processes and their interactions. Struct Saf 2018;72:99–110.
[41] Jia G, Gardoni P. Simulation-based approach for estimation of stochastic performances of deteriorating engineering systems. Probab Eng Mech 2018;52:28–39.
[42] Jia G, Gardoni P. Stochastic life-cycle analysis: Renewal-theory life-cycle analysis with state-dependent deterioration stochastic models. Struct Infrastruct Eng 2019;15(8):1001–14.
[43] Zaitseva E, Levashenko V. Investigation multi-state system reliability by structure function. In: 2nd International conference on dependability of computer systems. IEEE; 2007, p. 81–90.
[44] Kumar R, Gardoni P. Renewal theory-based life-cycle analysis of deteriorating engineering systems. Struct Saf 2014;50:94–102.
[45] Kumar R, Cline DB, Gardoni P. A stochastic framework to model deterioration in engineering systems. Struct Saf 2015;53:36–43.
[46] Volkanovski A, Čepin M, Mavko B. Application of the fault tree analysis for assessment of power system reliability. Reliab Eng Syst Saf 2009;94(6):1116–27.
[47] Fuchs CA, Van De Graaf J. Cryptographic distinguishability measures for quantum-mechanical states. IEEE Trans Inform Theory 1999;45(4):1216–27.